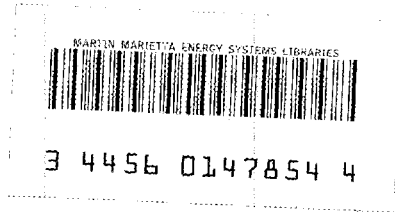


ornl

**OAK RIDGE
NATIONAL
LABORATORY**

MARTIN MARIETTA



ORNL/TM-10171

Helic Equilibria

T. C. Hender
B. A. Carreras
V. E. Lynch

OAK RIDGE NATIONAL LABORATORY
CENTRAL RESEARCH LIBRARY
CIRCULATION SECTION
OAK RIDGE, TENN.
LIBRARY LOAN COPY
DO NOT TRANSFER TO ANOTHER PERSON
If you wish someone else to see this
report, send in name with report and
the library will arrange a loan.

OPERATED BY
MARTIN MARIETTA ENERGY SYSTEMS, INC.
FOR THE UNITED STATES
DEPARTMENT OF ENERGY

Printed in the United States of America. Available from
National Technical Information Service
U.S. Department of Commerce
5285 Port Royal Road, Springfield, Virginia 22161
NTIS price codes—Printed Copy: A03; Microfiche A01

This report was prepared as an account of work sponsored by an agency of the United States Government. Neither the United States Government nor any agency thereof, nor any of their employees, makes any warranty, express or implied, or assumes any legal liability or responsibility for the accuracy, completeness, or usefulness of any information, apparatus, product, or process disclosed, or represents that its use would not infringe privately owned rights. Reference herein to any specific commercial product, process, or service by trade name, trademark, manufacturer, or otherwise, does not necessarily constitute or imply its endorsement, recommendation, or favoring by the United States Government or any agency thereof. The views and opinions of authors expressed herein do not necessarily state or reflect those of the United States Government or any agency thereof.

ORNL/TM-10171
Dist. Category UC-20g

Fusion Energy Division

HELIAC EQUILIBRIA

T. C. Hender*
B. A. Carreras
V. E. Lynch

*Present address: Culham Laboratory, Abingdon, Oxon, U.K.

Date Published: November 1986

Prepared by the
OAK RIDGE NATIONAL LABORATORY
Oak Ridge, Tennessee 37831
operated by
Martin Marietta Energy Systems, Inc.
for the
U.S. DEPARTMENT OF ENERGY
under Contract No. DE-AC05-84OR21400



3 4456 0147854 4

CONTENTS

ABSTRACT	v
1. INTRODUCTION	1
2. NUMERICAL METHODS	2
3. EQUILIBRIUM RESULTS	3
4. CONCLUSIONS AND DISCUSSION	18
5. ACKNOWLEDGMENTS	18
REFERENCES	19

ABSTRACT

Three-dimensional numerical calculations of Helic equilibria are presented. The results indicate that finite- β distortions in the flux surfaces can arise due to the presence of low order rational surfaces within or near the plasma. These distortions arise because of nonlinear beatings between the toroidal shift and the helical components of the magnetic field. Reducing the toroidal shift by increasing the number of field periods and/or the aspect ratio improves the equilibrium β -limit.

1. INTRODUCTION

The Heliac [1] consists of a toroidally directed central conductor, about which spirals a set of toroidal field (TF) coils. This coil set leads to an indented or "bean-shaped" plasma, whose magnetic axis follows the spiral motion of the TF coils. Figure 1 shows the coil set and magnetic surfaces at several toroidal locations for a four-field-period Heliac. Also included in the coil set are a pair of vertical field coils, which are necessary to control the horizontal position of the plasma.

ORNL-DWG 86-2593 FED

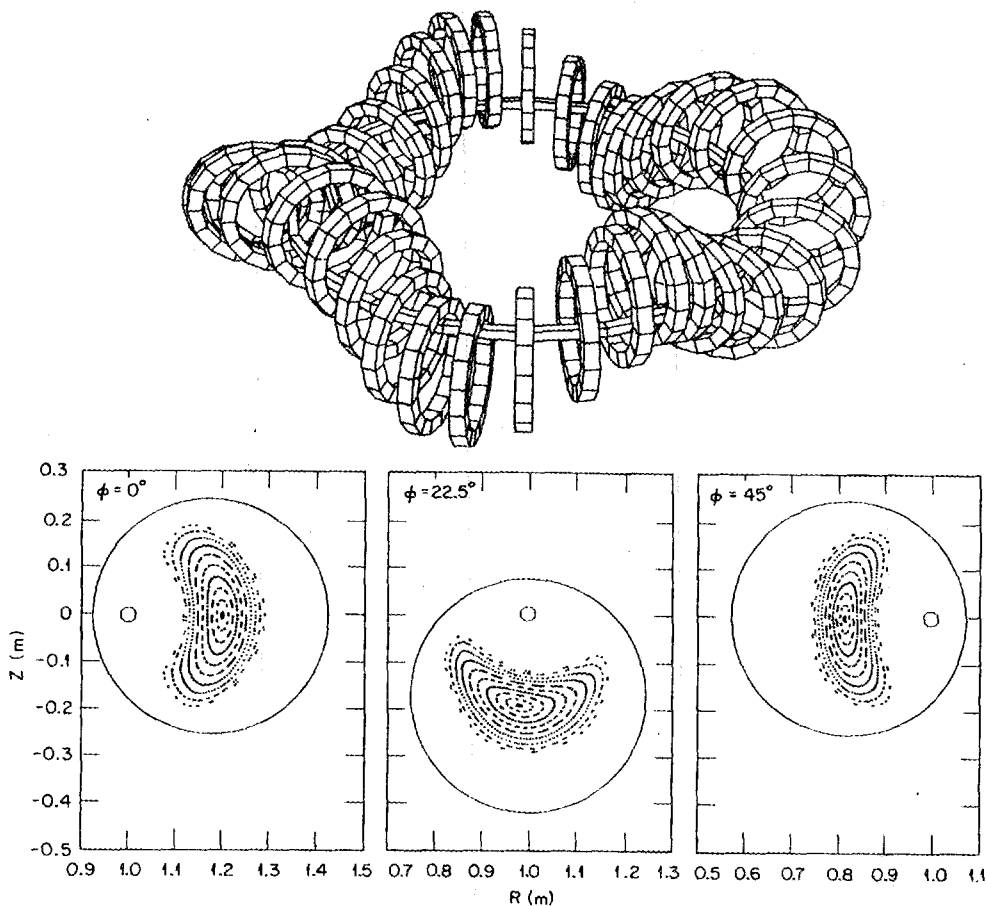


Fig. 1. Coil set and vacuum flux surfaces in constant toroidal angle planes for a four-field-period Heliac.

The strong helical curvature in the Heliac can lead to relatively deep magnetic wells and favorable stability properties. In the infinite aspect ratio, helically symmetric limit, the region of first stability to the ideal ballooning mode has been shown to extend to betas of at least 30%, for a relatively highly indented plasma [2].

To a more limited extent these results are also confirmed by stability calculations for finite aspect ratio HeliaCs [3]. The HeliaC thus appears to have good finite- β stability properties. The existence of toroidal equilibria at significant central beta values ($\beta_0 \sim 10\%$) is, however, questionable in many cases. In particular, at tight aspect ratio (i.e., strong toroidal curvature), the interplay between the toroidal and helical curvatures may lead at finite- β to resonant or nearly resonant harmonics, which can cause large distortions to the flux surfaces. The effect of these resonant harmonics is particularly accentuated by the low shear that is intrinsic to helical axis stellarators. Reimann and Boozer have given a first order analytic treatment of equilibrium flux surface destruction in the HeliaC [4]. For the particular case they examine, the $\iota/M = 0.5$ resonance is at the magnetic axis and a very low β -limit, $\beta \sim 0.5\%$, results. (Here ι is the rotational transform, and M is the number of field periods.) Cary and Kotschereuther have also made an analytic study of the effects of plasma pressure on equilibrium magnetic island formation in the stellarator [5]. Their results concentrate on the directly induced resonant Pfirsch-Schlüter currents and do not include higher order effects such as the beating of the toroidal and helical shifts. For configurations with high ι/M (such as the HeliaC), these beatings can lead directly to resonant harmonics and are thus important.

In this paper we present a mainly numerical study of toroidal HeliaC equilibria. These studies are performed with the three-dimensional (3-D) equilibrium code NEAR. In the next section, we give a brief review of NEAR. In Section 3 we present the equilibrium results, and finally, in Section 4, conclusions are given.

2. NUMERICAL METHODS

Full details have been given elsewhere of the 3-D equilibrium code NEAR [6]. In this section, we give only a brief summary of the code.

The 3-D NEAR code is based on a set of vacuum flux coordinates $(\rho_v, \theta_v, \phi_v)$ described by Boozer [7]. These coordinates are defined by their relationships to the vacuum magnetic field,

$$\vec{B}_v = B_0 \rho_v \vec{\nabla} \rho_v \times \vec{\nabla} (\theta_v - \iota_v \phi_v) = F_v \vec{\nabla} \phi_v \quad (1)$$

and by the additional constraints that $B_0 \rho_v^2 / 2$ is the vacuum toroidal flux and that the constant F_v should be such that ϕ_v varies by 2π in traversing the torus once toroidally. The $(\rho_v, \theta_v, \phi_v)$ coordinates and associated metric elements are derived numerically from given coil configurations, using the method described in Ref. [8].

The 3-D NEAR code uses the $(\rho_v, \theta_v, \phi_v)$ coordinates as its Eulerian frame of reference. The dependent variables are represented as doubly periodic Fourier series in the angular like variables θ_v and ϕ_v . Thus, for example, the contravariant component of the radial magnetic field is represented as

$$B^\rho(\rho_v, \theta_v, \phi_v, t) = \sum_{m,n} B^\rho(\rho_v, t) \sin(m\theta_v + n\phi_v) \quad (2)$$

This representation provides an accurate description of the small but important resonant harmonics. The equilibrium problem is solved, using this representation, by a steepest descent method in the manner described by Chodura and Schlüter [9]. A fictitious force \vec{F} is introduced,

$$\vec{F} = \vec{J} \times \vec{B} - \vec{\nabla}P \quad (3)$$

which in turn is related to a velocity \vec{V} by a conjugate gradient iteration scheme [9]. The magnetic field (\vec{B}) and pressure (P) are advanced subject to the constraints of flux and mass conservation:

$$\frac{\partial \vec{B}}{\partial t} = \nabla \times (\vec{V} \times \vec{B}) \quad (4)$$

and

$$\frac{\partial P}{\partial t} = -\vec{V} \cdot \vec{\nabla}P - \gamma P \nabla \cdot \vec{V} \quad (5)$$

where γ is the ratio of specific heats. It should be noted that the scheme makes no assumptions about the existence of good equilibrium flux surfaces, except at the last closed vacuum flux surface, where an infinitely conducting wall boundary condition is imposed. Advancing Eq. (4) directly leads to a flux conserving scheme (i.e., the vacuum ι profile as a function of toroidal flux is conserved during the iteration process). An additional iteration loop that has been added to the NEAR code also allows equilibria with zero net toroidal current to be calculated [10].

3. EQUILIBRIUM RESULTS

First we note that we study only cases in which good vacuum flux surfaces exist. This restriction is imposed directly by the need to be able to obtain the vacuum flux surface coordinates for the equilibrium calculation. It also seems a sensible prerequisite to require good vacuum flux surfaces. In the Helic, cases which contain or have nearby low order resonances ($\iota/M = 1/2, 1/3, \dots$) tend to have broken vacuum flux surfaces. Figure 2 shows the distortion and vacuum flux

surface destruction which occur for a case that cuts the $\nu/M = 1/3$ resonance. As we shall see, similar distortions of the flux surfaces can occur at finite- β for cases with good vacuum surfaces. The problem of finding good vacuum flux surfaces in the Heliac is caused partly by the low shear and also by generally high values of rotational transform per field period ($\nu/M \sim 0.5$), which make the low order resonances accessible.

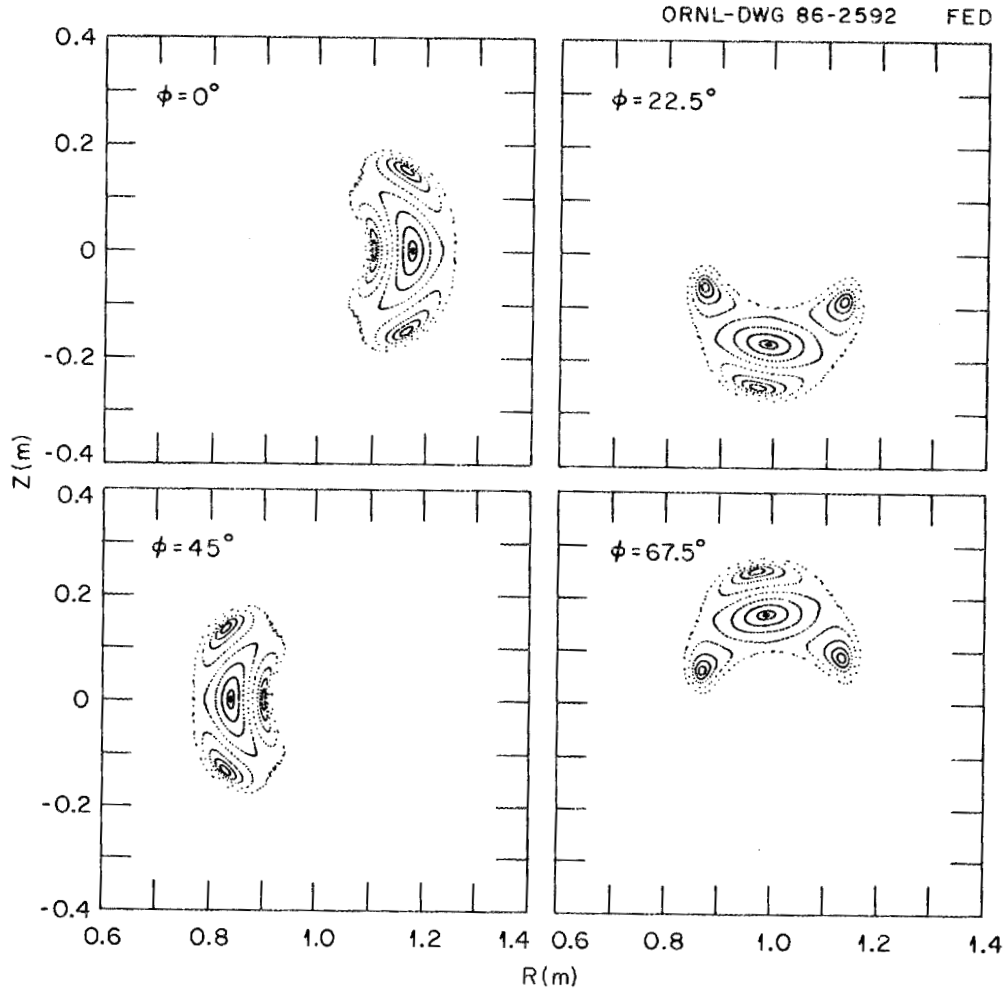


Fig. 2. Vacuum flux surfaces for a four-field-period case containing the $\nu/M = 1/3$ resonance.

To study the effects of finite- β on Heliac equilibria, we focus on cases which contain, or have nearby, the $\epsilon/M = 2/5$ resonance. Note that the resonance considered by Reimann and Boozer [4], $\epsilon/M = 0.5$, is a lower order and more damaging resonance than $2/5$. Figure 3 shows the vacuum and $\beta_0 = 5\%$ equilibrium flux surfaces calculated with the 3-D NEAR code for a four-field-period Heliac with a coil aspect ratio A_c of 4. The rotational transform in this case varies between 1.52 at the magnetic axis and 1.58 at the plasma edge. The equilibrium is flux conserving, and therefore its ϵ also varies over the same range. Distortions to the $\beta_0 = 5\%$ flux surfaces are evident in Fig. 3. By suppressing the contributions of given harmonics, we may examine the cause of these flux surface distortions. Figure 4 shows the flux surfaces for the $\beta_0 = 5\%$ case (Fig. 3) with the (5,8), (3,4), and (2,4) helicities removed. Suppressing the contributions of the (5,8) helicity lessens the distortion, and omitting the three helicities completely removes the distortions. In this case, the (5,8) harmonic is nearly resonant, so it strongly affects the flux surface quality. The (3,4) and (2,4) harmonics, although farther from being resonant with the ϵ range of plasma, are also important because they are lower order and thus larger than the (5,8) harmonic. At higher β , these distortions lead to a failure of convergence in the equilibrium code. Figure 5 shows the flux surfaces at $\beta_0 = 10\%$ after 2×10^5 and 8×10^5 iterations for the same case as Fig. 3. Eventually the distortions near the boundary become so large that they are incompatible with the fixed boundary constraint, and the code fails. Clearly, in this case a free boundary calculation is necessary to determine the existence of the equilibrium.

As discussed by Reimann and Boozer [4], there are two distinct mechanisms for the pressure-induced generation of these resonant or nearly resonant harmonics. First, there is the generation of the Pfirsch-Schlüter currents arising from the presence of the given harmonic in the vacuum spectrum. The radial magnetic field associated with these Pfirsch-Schlüter currents is given by

$$B_{m,n}^p = -\frac{|m|\beta_0}{a^2} \frac{\delta_{n,m}}{n - \epsilon m} \left[\frac{a^2}{4\rho_v} - \frac{\rho_v}{2} + \frac{\rho_v^3}{4a^2} + \frac{\rho_v}{2|m|+2} - \frac{\rho_v^3}{2(|m|+2)a^2} \right] + \frac{|m|\beta_0}{2a} \frac{\delta_{n,m}}{n - \epsilon m} \frac{1}{(|m|+1)(|m|+2)} \quad (7)$$

where $\delta_{n,m}$ is defined by

$$\frac{F_v}{B_v^2} = \frac{1}{B_0^2} \sum \delta_{n,m} \cos(m\theta_v + n\phi_v)$$

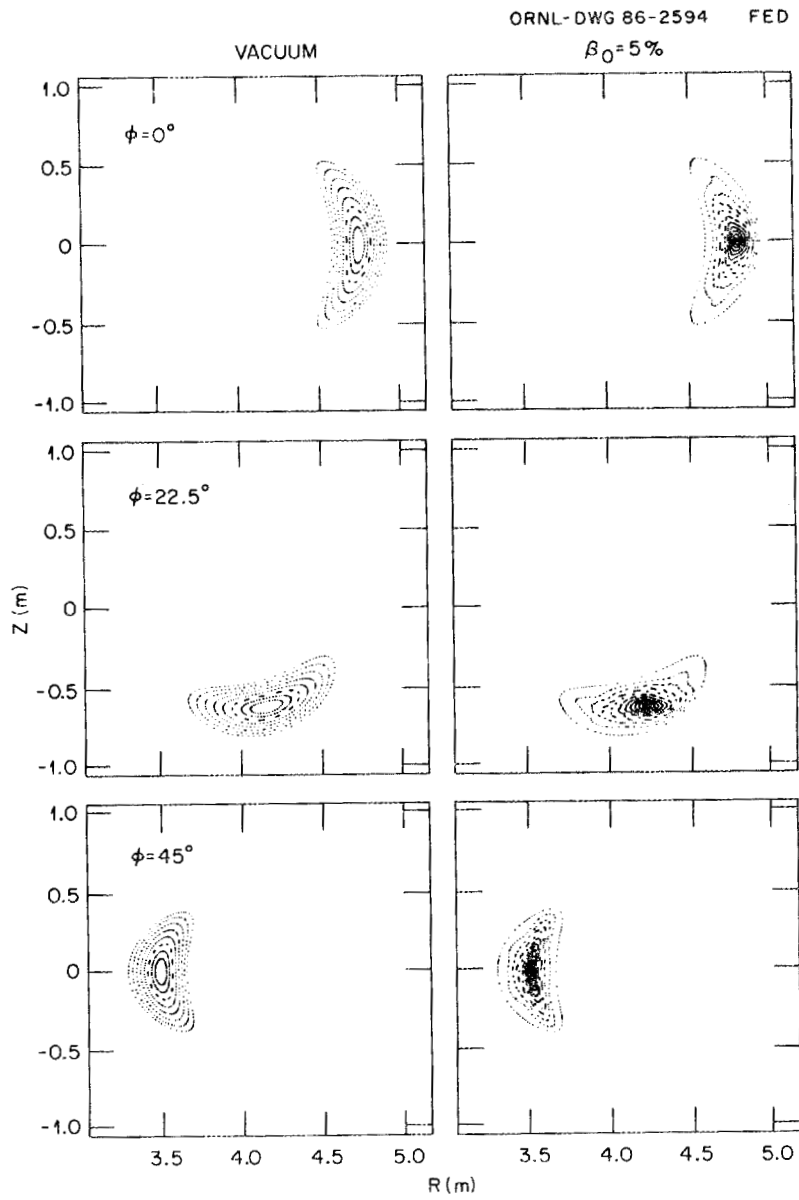


Fig. 3. Vacuum and $\beta_0 = 5\%$ flux surfaces for an $M = 4$ Helicoid with $1.52 \leq \nu \leq 1.58$.

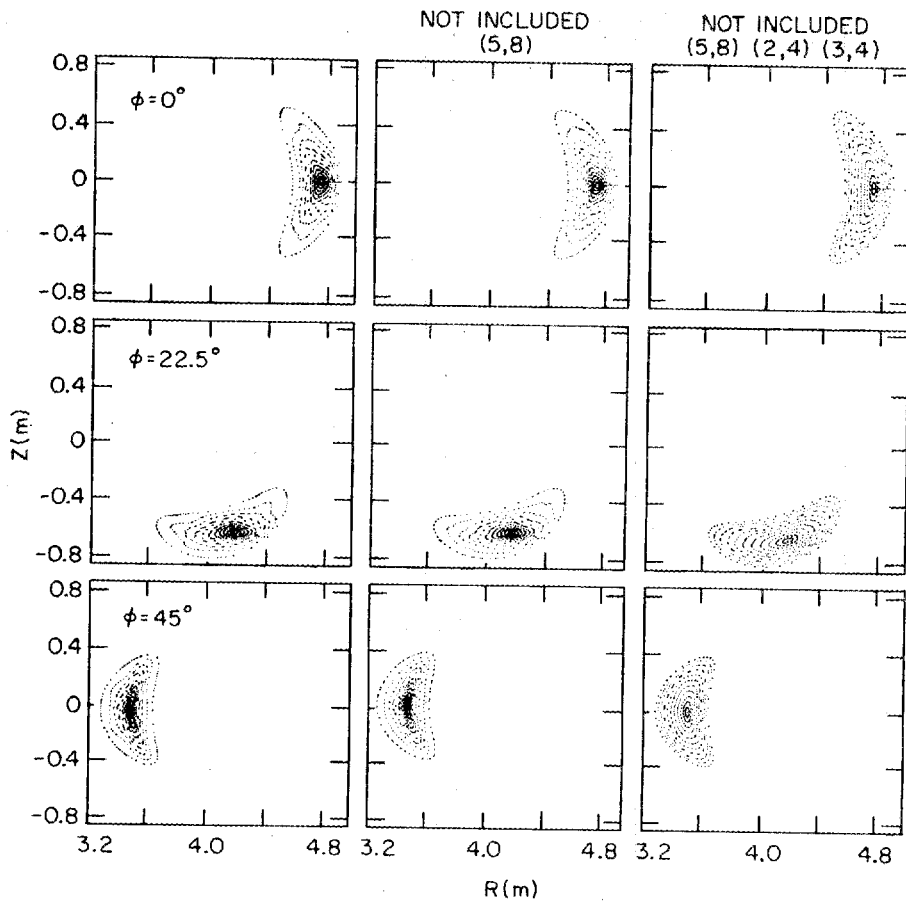


Fig. 4. Same case as Fig. 3 ($\beta_0 = 5\%$), showing that the (5,8), (3,4), and (2,4) helicities are the dominant mechanisms in causing the flux surface deformations.

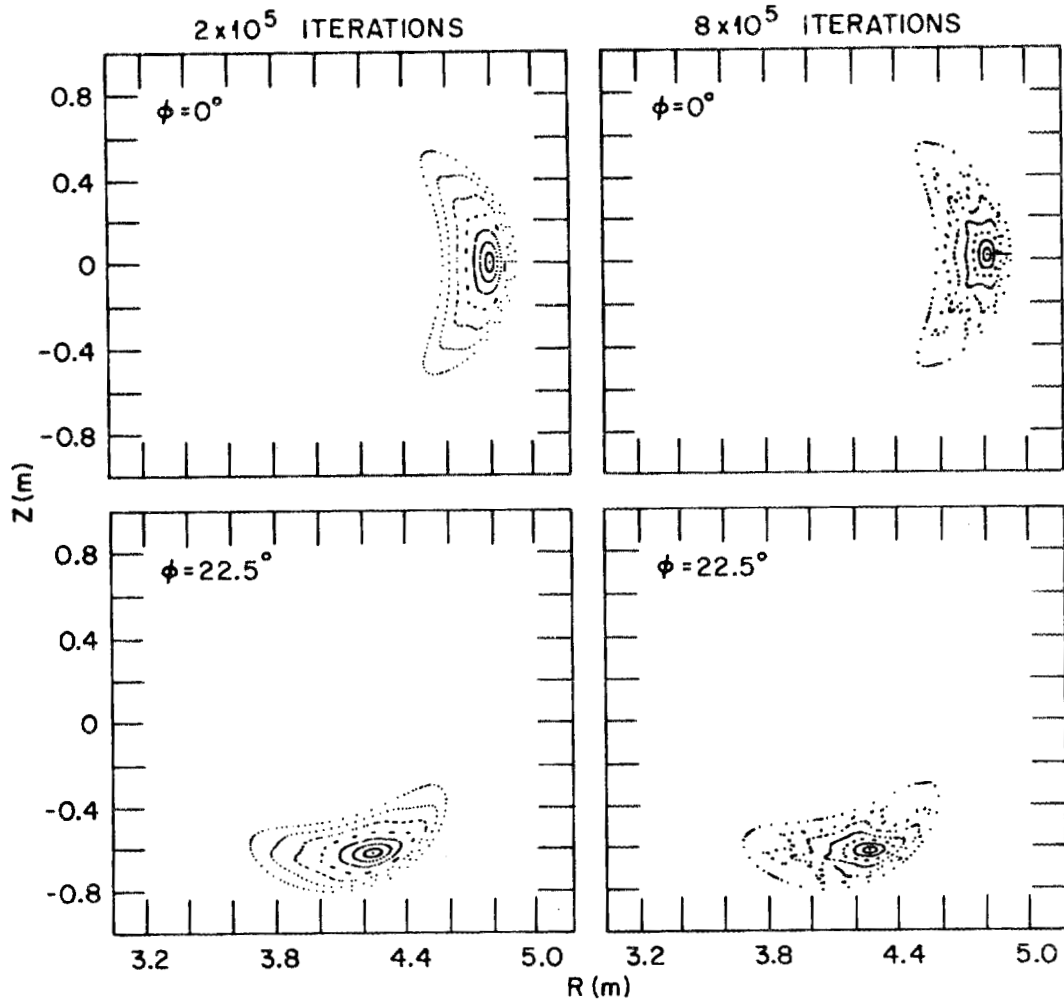


Fig. 5. Same case as Fig. 3, showing that the flux surface deformations grow without limit at $\beta_0 = 10\%$.

and the pressure profile is assumed to be $P = P_0[1 - (\rho_v/a)^2]^2$ with $\beta_0 = 2P_0/B_0^2$. Here $\rho_v = a$ is the location of an infinitely conducting wall. Comparing the radial magnetic field from Eq. (7) with the full numerical solution, we find that the Pfirsch-Schlüter currents account for about 30% of the (2,4) harmonic but are clearly unrelated to the generation of the (3,4) harmonic (Fig. 6). In contrast, there is very good agreement between the analytic and numerical (1,0) radial fields (upper plot, Fig. 6). Similarly good agreement exists with the helical (1,4) harmonic. As an alternative to using Eq. (7), we may run the FAR code with only the desired harmonic retained; the results are in good agreement with Eq. (7). For the (5,8) harmonic, the directly induced Pfirsch-Schlüter field is two orders of magnitude smaller than the numerically observed value. The dominant generation mechanism for these resonant or nearly resonant harmonics is the nonlinear beatings of low order harmonics. The case examined by Reimann and Boozer [4] relates to the nonlinear beatings of the toroidal (1,0) and helical (1, M) curvatures, which give rise to the (2, M) harmonic. In higher order such nonlinear beatings will lead to the generation of all possible harmonics (even if a harmonic is absent in the vacuum, i.e., its $\delta_{n,m} = 0$). These nonlinear beatings are present in all toroidal stellarators but are only important at very high β for $\ell = 2$ and 3 stellarators because of the relatively high shear and low ϵ/M (~ 0.1 typically) in these devices. In the Heliac, however, which has high ϵ/M and low shear, these nonlinearly induced resonant harmonics can become important at low β .

There are two obvious methods to reduce the finite- β flux surface distortions and increase the β -limit in the Heliac:

- (1) Choose the ϵ -range so as to avoid the dangerous low order resonances.
- (2) Decrease the magnitude of the nonlinear beatings that generate the resonant or nearly resonant harmonics.

Figure 7 shows the low order resonances for the range $1/2 \geq \epsilon/M \geq 1/4$ and $\beta_0 = 5\%$ flux conserving equilibria for three $A_c = 4$ Heliac configurations with the indicated ϵ -ranges. The case containing the $\epsilon/M = 2/5$ resonance is not fully converged, and eventually the flux surface distortions near the boundary cause the code to fail. This case and the case with the $2/5$ resonance nearby show very similar flux surface distortions. The case with $\epsilon/M \sim 0.36$ avoids the low order resonances ($m \leq 2$) and shows no flux surface distortions. For this case, however, at $\beta_0 = 10\%$, the $\epsilon/M = 3/8$ resonance gives rise to large $m = 8$ distortions to the flux surfaces. To alter the ϵ -ranges in these cases, we have varied the swing radii of the TF coils. For the standard Heliac (i.e., Fig. 1), varying the conductor currents gives very

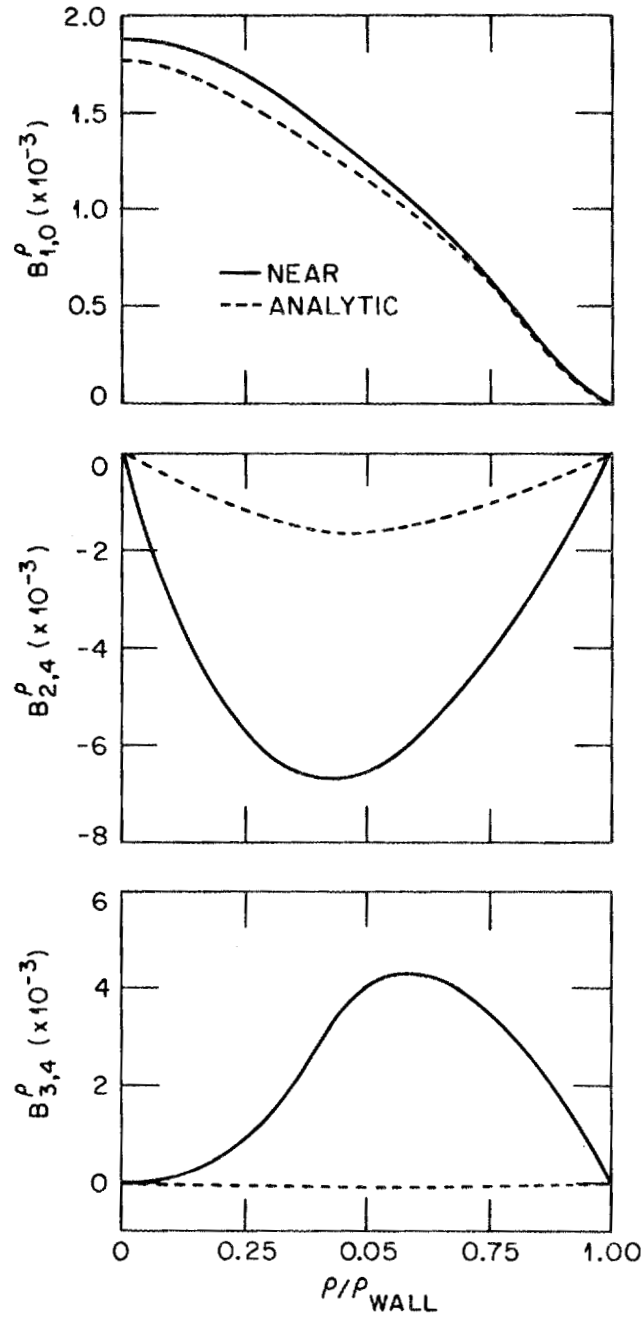


Fig. 6. Comparison of the analytic B^p associated with the Pfirsch-Schlüter currents and the full numerical solution for the (1,0), (2,4), (3,4) harmonics.

little freedom to vary ϵ , and it is generally necessary to change the geometry to alter ϵ significantly. For the Flexible Helic [11], however, where an additional $\ell = 1$ conductor is wrapped around the central conductor, extensive variation of ϵ can be achieved by varying the conductor currents. This allows the freedom for a single

For the equilibria shown so far, we have used the constraint of flux conservation. In stellarators with relatively low ϵ/M (~ 0.1), the constraint of zero net current can lead to relatively large finite- β deformations to the ϵ -profile [10]. In the Heliac, however, the high values of ϵ/M mean that the Pfirsch-Schlüter currents are small, and so the deformations to the ϵ -profile from the zero net current constraint are also correspondingly small. Figure 8 illustrates this for $\beta_0 = 5\%$ zero-current equilibria corresponding to the $\epsilon_0/M \sim 0.36$ case of Fig. 7. In this case, not only is the deformation to the ϵ -profile relatively small, but also the profile is within the range of ϵ values of the vacuum profile; thus the proximity of resonances (and associated flux surface deformations) is not greatly altered by the zero net current constraint.

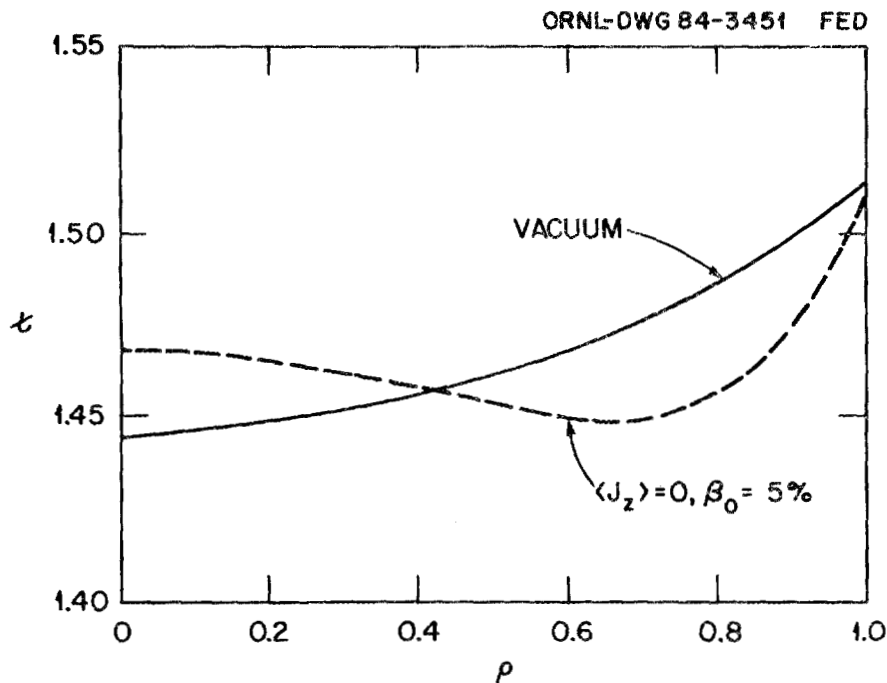


Fig. 8. Zero net current $\beta_0 = 5\%$ ϵ -profile for the $\epsilon/M = 0.36$ equilibria of Fig. 7.

The alternative method of reducing the finite- β flux surface distortions is to minimize the effect of the nonlinear beatings. As discussed above, the dominant harmonics which give rise to the nonlinear beatings are the toroidal $(1, 0)$ and helical $(1, M)$ shifts. Since the helical curvature is intrinsic to the Heliac design (and provides the magnetic well for good stability), minimizing the nonlinear beatings is essentially equivalent to minimizing the toroidal shift. The toroidal shift (Δ_T) varies as A_c/ϵ^2 . Thus, with an increase in the number of field periods at fixed aspect

ratio, ϵ increases as M , and the toroidal shift decreases as $1/M^2$. Alternatively, increasing the number of field periods and the aspect ratio in proportion causes the toroidal shift to decrease as $1/A_c$. Figures 9 and 10 compare the toroidal (Δ_T) and helical (Δ_H) shifts of a case with $M = A_c = 8$ with those of cases with $M = A_c = 12$ and $M = 16, A_c = 8$, respectively. Here Δ_T and Δ_H are defined by the relative shift between the vacuum magnetic axis (R_0, Z_0) and the finite- β magnetic axis (R_M, Z_M), as

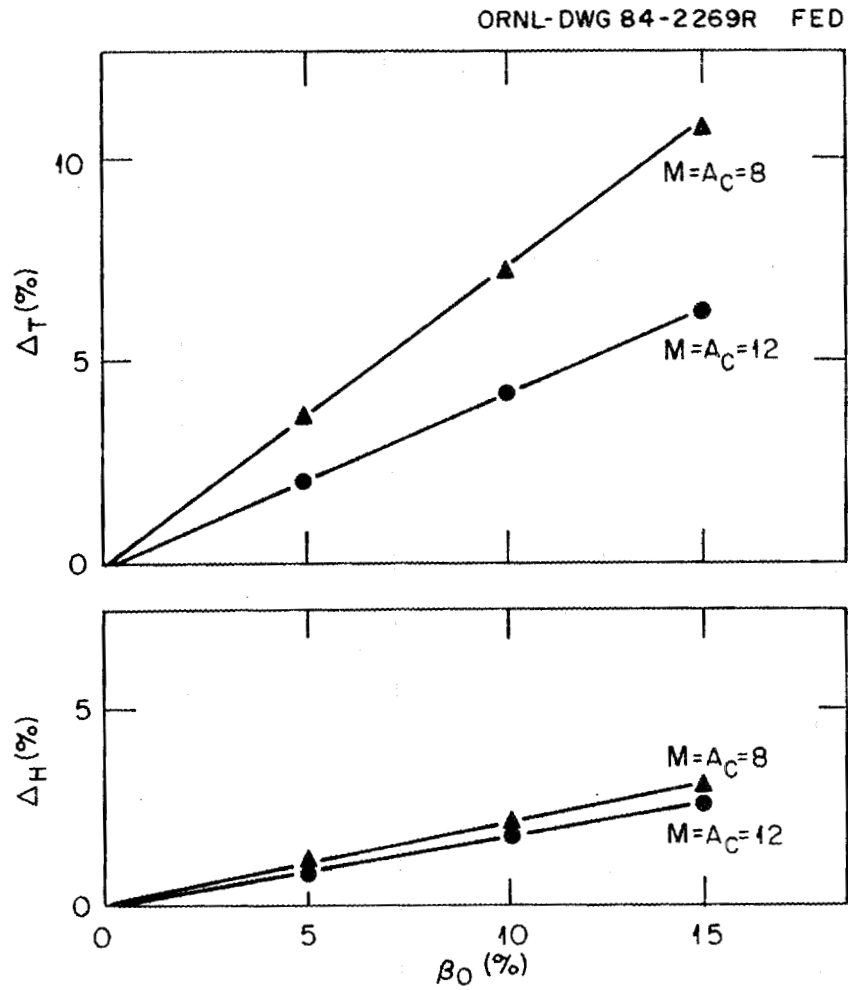


Fig. 9. Toroidal (Δ_T) and helical (Δ_H) shifts for an $M = A_c = 8$ and an $M = A_c = 12$ case with $\epsilon_0/M = 0.38$.

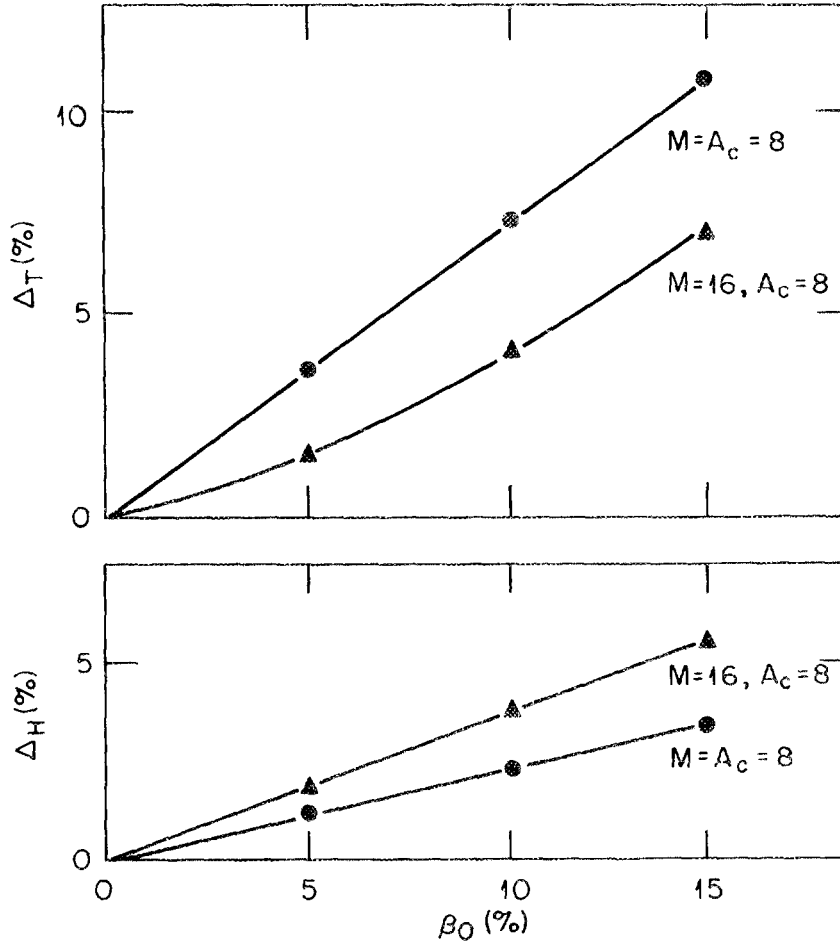


Fig. 10. Toroidal (Δ_T) and helical (Δ_H) shifts for an $M = A_c = 8$ case and an $M = 16$, $A_c = 8$ case with $\epsilon/M = 0.38$.

$$\Delta_T = \frac{1}{2\pi} \int_0^{2\pi} (R_M - R_0) d\phi$$

$$\Delta_H = \frac{1}{2\pi} \int_0^{2\pi} [(R_M - R_0) \cos M\phi + (Z_M - Z_0) \sin M\phi] d\phi$$

In Figs. 9 and 10 the $M = A_c$ cases have $\epsilon_0/M = 0.38$, whereas the $M = 2A_c$ case has $\epsilon_0/M = 0.42$. Both sequences are thus equidistant from the $\epsilon/M = 2/5$ resonance and should be affected similarly by the $(5, 2M)$ harmonic. From Fig. 9, we see that increasing M and A_c in proportion does decrease the toroidal shift as $1/A_c$ approximately. The underlying field period and the helical curvature are, however, unaffected by changing the number of field periods in this manner, and thus Δ_H

is practically invariant. Increasing the number of field periods at fixed A_c also produces the expected decrease in Δ_T (Fig. 10). In this case, however, we increase the helical curvature as we increase M , and so Δ_H becomes larger. The decrease in Δ_T with M shown in Fig. 10 is less than that expected analytically ($\Delta_T \propto 1/M^2$); this is probably because we must alter the coil geometry as we increase M , and this changes other factors which affect Δ_T . The decrease in Δ_T in these cases is reflected by an improvement of the equilibrium- β which can be achieved before the finite- β flux surface distortions occur. Figure 11 shows the $\beta_0 = 10\%$ flux surfaces for the $M = A_c = 12$ and $M = 16, A_c = 8$ cases. At very high β ($\sim 20\%$) these cases also suffer from large-scale distortions of the flux surfaces due to the proximity of the $r/M = 2/5$ resonance.

We have also investigated methods for reducing the toroidal shift at fixed M and A_c . These methods rely on reducing the toroidal $\delta_{0,1}$ harmonic, which is directly related to the toroidal shift [see Eq. (7)]. In lowest order, this term is determined by the $1/R$ dependence, due to the chosen A_c , and so at fixed A_c we can only affect $\delta_{0,1}$ by higher order nonlinear beatings. We have examined two methods of altering $\delta_{0,1}$:

- (1) Modulate the TF coil winding law according to $\theta = M\phi + C_M \sin M\phi$.
- (2) Modulate the TF coil currents according to $I = I_0(1 + C_F \cos M\phi)$.

These methods produce very similar results. By modulating the winding law or currents in this manner we are directly affecting the $(0, M)$ harmonic [which by beating with the $(1, M)$ helical harmonic alters the $(1, 0)$ harmonic]. Unfortunately, at $A_c = 4$ these modulations cannot be made large enough to have any significant impact on the $\delta_{0,1}$ harmonic, which is totally dominated by the $1/R$ terms. Figure 12 illustrates this for an $A_c = 4$ case by showing a wide range of variation of the $(0, 4)$ harmonic with the current modulation (C_F) while the $(1, 0)$ harmonic is practically invariant. Since the toroidal shift is directly related to the $\delta_{0,1}$ harmonic there is no appreciable change in the finite- β flux surface deformations resulting from current or winding law modulations (for small A_c). At larger aspect ratio ($A_c \sim 20$), reductions of $\sim 30\%$ in Δ_T can be achieved by modulating current. This is because the $1/R$ terms are weaker and the $\delta_{0,1}$ harmonic can be affected by nonlinear beatings.

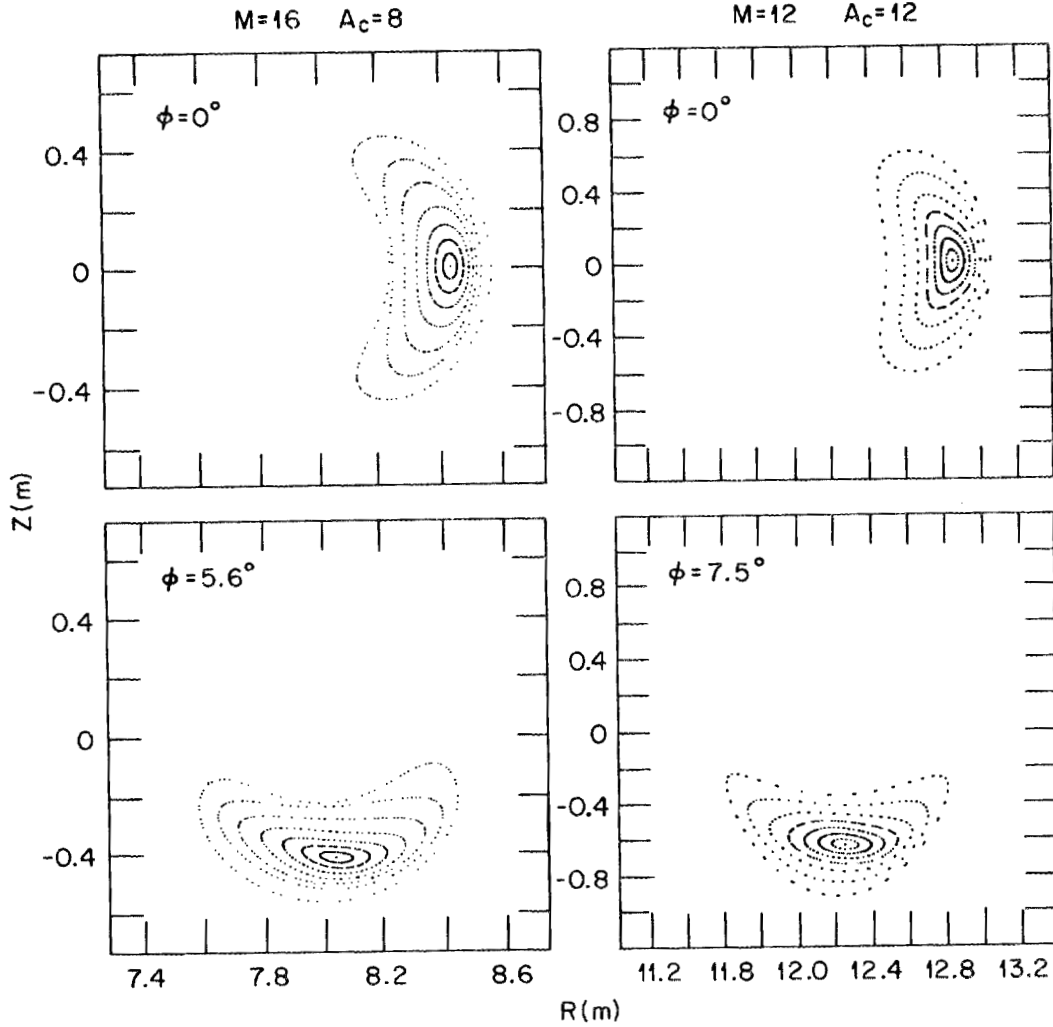


Fig. 11. $\beta_0 = 10\%$ equilibrium flux surfaces for the $M = A_c = 12$ and $M = 16$, $A_c = 8$ cases of Figs. 9 and 10.

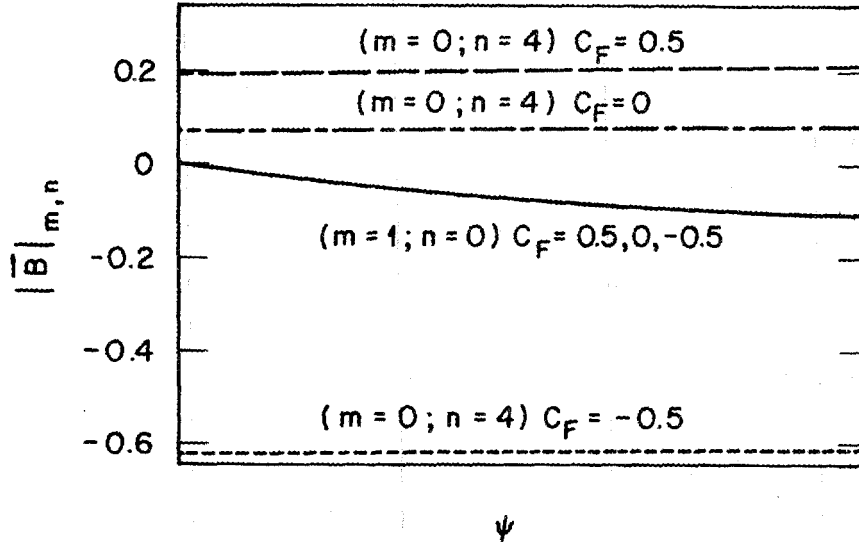


Fig. 12. Variation of the $|\vec{B}|_{0,4}$ and $|\vec{B}|_{1,0}$ vacuum harmonics with the TF coil current modulation (C_F). [The (1,0) harmonic changes so little that only one curve is shown.]

4. CONCLUSIONS AND DISCUSSION

Calculations of fully 3-D Helicac equilibria with the NEAR code have been presented. The results, which confirm the analytic calculation of Reimann and Boozer, show that the presence of low order resonant surfaces in or near the plasma can lead to the finite- β destruction of equilibrium flux surfaces. The results are also in qualitative agreement with numerical calculations by Park et al. [12] on the effects of the $\iota/M = 0.5$ resonance. The effects of low order resonances in the Helicac are greatly accentuated by the low shear and high ι/M , which make the low order resonances accessible. For the particular resonance studied in this paper, $\iota/M = 2/5$, the dominant mechanism for generating the resonant harmonic $(5, 2M)$ is the nonlinear beatings of low order harmonics, the largest of which are the toroidal and helical shifts. Since the helical curvature is intrinsic to the Helicac design, we can only minimize the nonlinear beatings, which give rise to the resonant harmonics by reducing the finite- β toroidal shift. At tight aspect ratio ($A_c = 4$), the toroidal shift is large and the finite- β deformation of the flux surfaces becomes very large for $\beta_0 \geq 5\%$. By increasing the number of field periods and/or the aspect ratio, we reduce the toroidal shift and raise the equilibrium β -limit. For $M = A_c = 12$, configurations with good equilibria have been found up to at least $\beta_0 = 10\%$. At fixed aspect ratio and number of field periods we can optimize the equilibrium beta by tuning the ι -range to avoid the low order rational surfaces. At fixed M and A_c we have also investigated methods for reducing the toroidal shift by modulating the TF coil winding law or currents. At tight aspect ratio ($A_c \sim 4$), these modulations are unable to overcome the intrinsic $1/R$ toroidicity and there is no reduction in Δ_T or corresponding improvement in the finite- β flux surface destruction. At larger aspect ratio ($A_c \sim 20$), however, a modest reduction ($\sim 30\%$) in Δ_T results from modulating the TF coil currents.

5. ACKNOWLEDGMENTS

We are indebted to J. A. Rome and J. H. Harris for assistance and encouragement with these calculations. We also thank A. Reimann and A. H. Boozer for several useful discussions.

REFERENCES

- [1] BOOZER, A. H., CHU, T. K., DEWAR, R. L., FURTH, H. P., GORCE, J. A., JOHNSON, J. L., KULSRUD, R. M., MONTICELLO, D. A., KUO-PETRAVIC, G., SHEFFIELD, G. V., YOSHIKAWA, S., BETANCOURT, O., in *Plasma Physics and Controlled Nuclear Fusion Research 1982 (Proc. 9th Int. Conf. Baltimore, 1982) Vol. 3*, IAEA, Vienna (1983) 129.
- [2] MONTICELLO, D. A., DEWAR, R. L., FURTH, H. P., REIMANN, A., *Phys. Fluids* **27** (1984) 1248.
- [3] BAUER, F., BETANCOURT, O., GARABEDIAN, P., *Magnetohydrodynamic Equilibrium and Stability of Stellarators*, Springer-Verlag, New York (1984).
- [4] REIMANN, A., BOOZER, A. H., *Phys. Fluids* **27** (1984) 2446.
- [5] CARY, J. R., KOTSCHEREUTHER, M., *Phys. Fluids* **28** (1985) 1392.
- [6] HENDER, T. C., CARRERAS, B. A., GARCIA, L., ROME, J., LYNCH, V. E., *J. Comput. Phys.* **60** (1984) 76.
- [7] BOOZER, A. H., *Phys. Fluids* **25** (1982) 520.
- [8] KUO-PETRAVIC, G., BOOZER, A. H., ROME, J. A., FOWLER, R. H., *J. Comput. Phys.* **51** (1983) 261.
- [9] CHODURA, R., SCHLÜTER, A., *J. Comput. Phys.* **41** (1981) 68.
- [10] HENDER, T. C., CARRERAS, B. A., CHARLTON, L. A., GARCIA, L., HICKS, H. R., HOLMES, J. A., LYNCH, V. E., *Nucl. Fusion* **25** (1985) 1463.
- [11] HARRIS, J. H., CANTRELL, J. L., HENDER, T. C., CARRERAS, B. A., MORRIS, R. N., *Nucl. Fusion* **25** (1985) 623.
- [12] PARK, W., MONTICELLO, D. A., STRAUSS, H. R., and MANICKAM, J., *Phys. Fluids* **29** (1986) 1171.

INTERNAL DISTRIBUTION

- | | | | |
|--------|-------------------|--------|--------------------------------|
| 1. | L. A. Berry | 18. | Y-K. M. Peng |
| 2-3. | B. A. Carreras | 19. | J. Sheffield |
| 4. | R. A. Dory | 20. | D. J. Sigmar |
| 5. | J. Dunlap | 21-22. | Laboratory Records Department |
| 6. | H. Haselton | 23. | Laboratory Records, ORNL-RC |
| 7. | P. N. Haubenreich | 24. | ORNL Patent Office |
| 8. | C. L. Hedrick | 25. | Document Reference Section |
| 9-13. | T. C. Hender | 26. | Central Research Library |
| 14. | J. T. Hogan | 27. | Fusion Energy Division Library |
| 15. | M. S. Lubell | 28. | Fusion Energy Division |
| 16-17. | V. E. Lynch | | Publications Office |

EXTERNAL DISTRIBUTION

29. Office of the Assistant Manager for Energy Research and Development, Department of Energy, Oak Ridge Operations Office, P. O. Box E, Oak Ridge, TN 37831
30. J. D. Callen, Department of Nuclear Engineering, University of Wisconsin, Madison, WI 53706
31. R. W. Conn, Department of Chemical, Nuclear, and Thermal Engineering, University of California, Los Angeles, CA 90024
32. S. O. Dean, Director, Fusion Energy Development, Science Applications International Corporation, 2 Professional Drive, Suite 249, Gaithersburg, MD 20760
33. H. K. Forsen, Bechtel Group, Inc., Research Engineering, P. O. Box 3965, San Francisco, CA 94105
34. A. Fruchtman, Courant Institute of Mathematical Sciences, New York University, 251 Mercer Street, New York, NY 10012
35. R. W. Gould, Department of Applied Physics, California Institute of Technology, Pasadena, CA 91125
36. D. G. McAlees, Exxon Nuclear Co., Inc., 777 106th Avenue, NE, Bellevue, WA 98009
37. K. Riedel, Courant Institute of Mathematical Sciences, New York University, New York, NY 10012
38. H. Weitzner, Courant Institute of Mathematical Sciences, New York University, New York, NY 10012

39. P. J. Reardon, Princeton Plasma Physics Laboratory, P. O. Box 451, Princeton, NJ 08544
40. W. M. Stacey, School of Nuclear Engineering, Georgia Institute of Technology, Atlanta, GA 30332
41. G. A. Eliseev, I. V. Kurchatov Institute of Atomic Energy, P. O. Box 3402, 123182 Moscow, U.S.S.R.
42. V. A. Glukhikh, Scientific-Research Institute of Electro-Physical Apparatus, 188631 Leningrad, U.S.S.R.
43. I. Spighel, Lebedev Physical Institute, Leninsky Prospect 53, 117924 Moscow, U.S.S.R.
44. D. D. Ryutov, Institute of Nuclear Physics, Siberian Branch of the Academy of Sciences of the U.S.S.R., Sovetskaya St. 5, 630090 Novosibirsk, U.S.S.R.
45. V. T. Tolok, Kharkov Physical-Technical Institute, Academical St. 1, 310108 Kharkov, U.S.S.R.
46. R. Varma, Physical Research Laboratory, Navangpura, Ahmedabad, India
47. Bibliothek, Max-Planck Institut fur Plasmaphysik, D-8046 Garching bei Munchen, Federal Republic of Germany
48. Bibliothek, Institut fur Plasmaphysik, KFA, Postfach 1913, D-5170 Julich, Federal Republic of Germany
49. Bibliotheque, Centre des Recherches en Physique des Plasmas, 21 Avenue des Bains, 1007 Lausanne, Switzerland
50. Bibliotheque, Service du Confinement des Plasmas, CEA, B.P. No. 6, 92 Fontenay-aux-Roses (Seine), France
51. Documentation S.I.G.N., Departement de la Physique du Plasma et de la Fusion Controlee, Centre d'Etudes Nucleaires, B.P. 85, Centre du Tri, 38041 Cedex, Grenoble, France
52. Library, Culham Laboratory, UKAEA, Abingdon, Oxon, OX14 3DB, England
53. Library, FOM-Instituut voor Plasma-Fysica, Rijnhuizen, Jutphaas, The Netherlands
54. Library, Institute of Physics, Academia Sinica, Beijing, Peoples Republic of China
55. Library, Institute of Plasma Physics, Nagoya University, Nagoya, Japan
56. Library, International Centre for Theoretical Physics, Trieste, Italy
57. Library, Laboratorio Gas Ionizzati, Frascati, Italy
58. Library, Plasma Physics Laboratory, Kyoto University, Gokasho Uji, Kyoto, Japan
59. Plasma Research Laboratory, Australian National University, P.O. Box 4, Canberra, A.C.T. 2000, Australia
60. Thermonuclear Library, Japan Atomic Energy Research Institute, Tokai, Naka, Ibaraki, Japan

61. J. F. Clarke, Associate Director for Fusion Energy, Office of Fusion Energy, Office of Energy Research, U.S. Department of Energy, Mail Stop G-256, Washington, DC 20545
62. D. B. Nelson, Acting Director, Division of Applied Plasma Physics, Office of Fusion Energy, Office of Energy Research, U.S. Department of Energy, Mail Stop G-256, Washington, DC 20545
63. W. Sadowski, Fusion Theory and Computer Services Branch, Office of Fusion Energy, Office of Energy Research, U.S. Department of Energy, Mail Stop G-256, Washington, DC 20545
64. N. A. Davies, Tokamak Systems Branch, Office of Fusion Energy, Office of Energy Research, U.S. Department of Energy, Mail Stop G-256, Washington, DC 20545
65. E. Oktay, Tokamak Systems Branch, Office of Fusion Energy, Office of Energy Research, U.S. Department of Energy, Mail Stop G-256, Washington, DC 20545
66. M. N. Rosenbluth, University of Texas, Institute for Fusion Studies, RLM 11.218, Austin, TX 78712
67. Theory Department Read File, c/o D. W. Ross, University of Texas, Institute for Fusion Studies, Austin, TX 78712
68. Theory Department Read File, c/o R. C. Davidson, Director, Plasma Fusion Center, NW 16-202, Massachusetts Institute of Technology, Cambridge, MA 02139
69. Theory Department Read File, c/o F. W. Perkins, Princeton Plasma Physics Laboratory, P.O. Box 451, Princeton, NJ 08544
70. Theory Department Read File, c/o L. Kovrizhnikh, Lebedev Institute of Physics, Academy of Sciences, 53 Leninsky Prospect, 117924 Moscow, U.S.S.R.
71. Theory Department Read File, c/o B. B. Kadomtsev, I. V. Kurchatov Institute of Atomic Energy, P.O. Box 3402, 123182 Moscow, U.S.S.R.
72. Theory Department Read File, c/o T. Kamimura, Institute of Plasma Physics, Nagoya University, Nagoya, Japan
73. Theory Department Read File, c/o C. Mercier, Euratom-CEA, Service des Recherches sur la Fusion Controlee, Fontenay-aux-Roses (Seine), France
74. Theory Department Read File, c/o T. E. Stringer, JET Joint Undertaking, Culham Laboratory, Abingdon, Oxon OX14 3DB, England
75. Theory Department Read File, c/o K. Roberts, Culham Laboratory, Abingdon, Oxon OX14 3DB, England
76. Theory Department Read File, c/o D. Biskamp, Max Planck Institut fur Plasmaphysik, D-8046 Garching bei Munchen, Federal Republic of Germany
77. Theory Department Read File, c/o T. Takeda, Japan Atomic Energy Research Institute, Tokai, Naka, Ibaraki, Japan

78. Theory Department Read File, c/o C. S. Liu, GA Technologies, Inc., P.O. Box 81608, San Diego, CA 92138
79. Theory Department Read File, c/o L. D. Pearlstein, Lawrence Livermore National Laboratory, P.O. Box 808, Livermore, CA 94550
80. Theory Department Read File, c/o R. Gerwin, CTR Division, Los Alamos National Laboratory, P.O. Box 1663, Los Alamos, NM 87545
81. T. Amano, Institute of Plasma Physics, Nagoya University, Nagoya, Japan
82. C. D. Boley, Fusion Power Program, Building 207C, Argonne National Laboratory, Argonne, IL 60439
83. Yu. N. Dnestrovskii, I. V. Kurchatov Institute of Atomic Energy, P.O. Box 3402, 123182 Moscow, U.S.S.R.
84. J. Gaffey, IPST, University of Maryland, College Park, MD 20742
85. R. J. Hawryluk, Princeton Plasma Physics Laboratory, P.O. Box 451, Princeton, NJ 08544
86. W. W. Pfeiffer, GA Technologies, Inc., P.O. Box 81608, San Diego, CA 92138
87. D. E. Post, Princeton Plasma Physics Laboratory, P.O. Box 451, Princeton, NJ 08544
88. A. Ware, Physics Department, University of Texas, Austin, TX 78712
89. J. Wiley, University of Texas, Institute for Fusion Studies, Austin, TX 78712
90. S. K. Wong, GA Technologies, Inc., P.O. Box 81608, San Diego, CA 92138
91. S. Yoshikawa, Princeton Plasma Physics Laboratory, P.O. Box 451, Princeton, NJ 08544
- 92-243. Given distribution as shown in TID-4500, Magnetic Fusion Energy (Category UC-20g, Theoretical Plasma Physics)